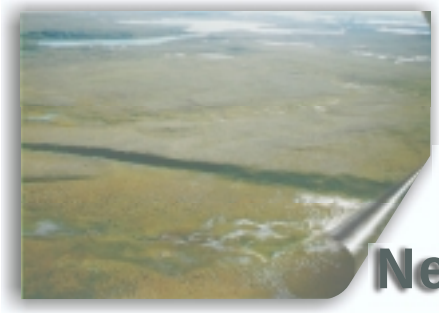

NEONOR
Neotectonics in Norway

NGU Report 99.082
Neotectonic excursion guide to
Troms and Finnmark

CONTENTS

MAP ENCLOSURES

Bedrock map, Scale 1:50.000, 1933 IV Masi, (Solli 1988)

Bedrock map Scale, 1:500.000 Finnmark, (Siedlecka & Roberts 1996)

Geophysical maps, Scale 1:1 mill. Western Finnmark and northern Troms, (Olesen et al. 1990)

1. INTRODUCTION: LAPLAND POSTGLACIAL FAULT PROVINCE

The Stuoragurra Fault (SF) is part of the Lapland province of postglacial faults and was identified in 1983 during the course of a collaborative project between the Geological Surveys of Finland, Norway and Sweden. Details on the Stuoragurra Fault have been reported by Olesen (1988, 1991), Muir Wood (1989), Olesen et al. (1992a,b) and Roberts et al. (1997). Bungum & Lindholm (1997) carried out a detailed seismotectonic study. The southernmost part of the Stuoragurra Fault has also been included in the Masi bedrock map at the scale 1:50.000 by Solli (1988).

Similar NNE-SSW trending reverse faults occur in adjacent parts of Finland (Kujansuu 1964) and Sweden (Lundqvist & Lagerbäck 1976, Lagerbäck 1979, 1990) within a 400x400 km large area. The Pärve Fault is up to 150 km in length. The Lainio-Suijavaara Fault has an escarpment 30 m in height. The major faults are NE-SW trending reverse faults while the two minor faults, the Nordmannvikdalen and Vaalajärvi faults, have a NNW-SSE direction which is perpendicular to the trend of the reverse faults. The Nordmannvikdalen fault in northern Troms is a normal fault. The dip of the parallel Vaalajärvi Fault in northern Finland is not known, but ground penetrating radar (GPR) measurements indicate a normal fault (Mauring et al. 1999). Kakkuri & Chen (1992) mapped recent crustal extension in NE-SW direction from triangulation data in this area.

The University of Tromsø and the Geological Institute of Kola Science Centre have carried out a study of the Holocene shorelines, on the Rybachi and Sredny Peninsulas (Corner et al. 1999, Yevzerov et al. 1998). Levelling of shorelines did not confirm that there are postglacial faults between Rybachi and Sredny as proposed by Tanner (1907). Marthinussen (1974) did also question the proposed postglacial age of these faults. The Vuotso and Kelottijärvi faults in northern Finland have been subject to more detailed studies in recent years and are found not to be of postglacial age (Kuivamäki et al. 1998).

Taking into account the classification of neotectonic claims in Norway by Dehls & Braathen (1998) and Olesen & Dehls (1998), in Finland by Kuivamäki et al. (1998) and in Sweden by Muir Wood (1993) we may conclude that most of the well documented (grade A) postglacial faults in Fennoscandia occur within the Lapland Fault Province (Table 1). There are, however, a few examples of postglacial faults in southern Scandinavia, e.g. in the Norwegian Trench as reported by Hovland (1983).

*Table 1. Summary of properties of the documented postglacial faults within the Lapland province. The major faults are NE-SW trending reverse faults and occur within a 400x400 km large area in northern Fennoscandia. The Nordmannvikdalen and Vaalajärvi faults are minor faults trending perpendicular to the reverse faults. The former is a normal fault and the latter is a potential normal fault. The scarp height/length ratio is generally less than 0.001. The Merasjärvi Fault has a scarp height/length ratio of 0.002. *Moment magnitudes calculated from fault offset and length utilising formulas by Wells and Coppersmith (1994).*

Fault	Country	Length (km)	Max. scarp height (m)	Height length ratio	Trend	Type	Moment magni-tude*	Comment	Reference
Suasselkä Fault	Finland	48	5	0.0001	NE-SW	reverse	7.0		Kujansuu, 1964
Pasmajärvi-Venejärvi Fault	Finland	15	12	0.0008	NE-SW	reverse	6.5	two separate sections	Kujansuu, 1964
Vaalajärvi Fault	Finland	6	2	0.0003	NW-SE	??	6.0		Kujansuu, 1964
Pärve Fault	Sweden	150	13	0.0001	NE-SW	reverse	7.6		Lundquist & Lagerbäck, 1976
Lainio-Suijavaara Fault	Sweden	55	30	0.0005	NE-SW	reverse	7.1		Lagerbäck, 1979
Merasjärvi Fault	Sweden	9	18	0.002	NE-SW	reverse	6.3		Lagerbäck, 1979
Pirttimys Fault	Sweden	18	2	0.0001	NE-SW	reverse	6.5		Lagerbäck, 1979
Lansjärv Fault	Sweden	50	22	0.0004	NE-SW	reverse	7.1		Lagerbäck, 1979
Burträsk-Bastuträsk Fault	Sweden	60	c. 10	0.0002	NE-SW N-S	??	7.1	two separate sections	Lagerbäck, 1979
Stuoragurra Fault	Norway	80	7	0.0001	NE-SW	reverse	7.3	Three separate sections	Olesen, 1988
Nordmannvik-dalen Fault	Norway	3	1	0.0003	NW-SE	normal	5.7		Tolgensbakk & Sollid, 1988

The Lapland province of reverse postglacial faults constitutes one of five major components of Neogene tectonics in western Fennoscandia:

1) Uplift and exhumation of the mainland and the Barents Sea

2) Neogene (late Miocene?) reactivation of domes and arches offshore Mid-Norway (originally formed in the Eocene)

3) The offshore deposition of large Pliocene-Pleistocene propagating wedges

4) Glaciation/deglaciation cycles throughout the late Neogene

5) The Lapland province of reverse postglacial faults

It is still uncertain which of these elements are linked to each other and how they may be linked genetically. Are the large offshore domes and arches and the offshore propagating wedges genetically linked to the Lapland fault province? Is the ridge-push force associated with the rifting along the Mohns and Knipovich Ridges, the initiating mechanism for the Neogene tectonics, or are the deteriorating climate and onset of glaciations a dominant agent. Since the formation of the offshore domes and arches was initiated in Eocene, it is natural to relate these features to a ridge-push force. It is, however, still an open question whether the postglacial faults are caused by this ridge-push force or the major strain release immediately following glacial unloading or a possible combination of these effects. Muir Wood (1993) has summarised the latter model in Fig. 1. Riis (1996) constrained the Neogene uplift to a Pleistocene tectonic phase which operated the last 1 Ma. This event caused subsidence of the Norwegian Channel and uplift of the south Norway mountain plateau. Similarly, the Lofoten area seems to be an area of recent vertical movement. Riis (1996) relates this tectonic phase to the change in glaciation intensity and cyclicity at 1Ma and modification of sedimentation and ice loads afterwards. Stuevold & Eldholm (1996) advocate that the intraplate deformation is an effect of a deep-seated thermal source.

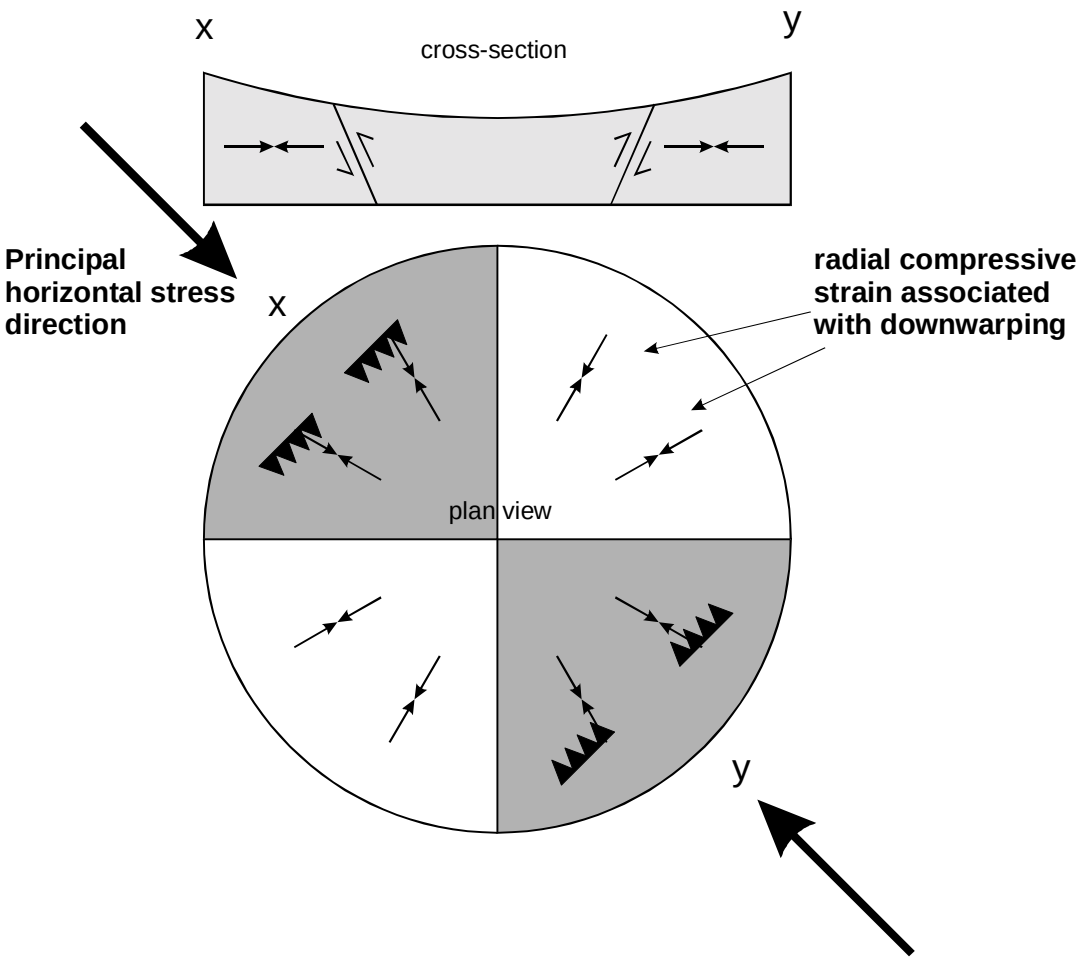

Figure 1. Model for the concentration of major strain release immediately following rapid glacial unloading proposed by Muir Wood (1993). Assuming a circular ice-cap located on a flat laterally homogenous crust, the flanks of the downwarped crust will have suffered a radial increase in stress during glacial loading. On the flanks of the downwarped bowl facing the principal horizontal stress direction (ridge-push stress oriented NW-SE in Scandinavia), radial strain raises sigma 1 during downwarping, and on glacial unloading this will cause postglacial faulting. This model will explain the reverse faults within the Lapland Province, but not the normal faults. The model would also imply postglacial faulting to the southeast of the rebound dome in Finland where postglacial faults have not been observed.

1.1 The Stuoragurra Fault

The Stuoragurra Fault (SF), located within the Mierujavri Sværholt Fault Zone (MSFZ), is an 80 km long fault zone (Fig. 2) which contains three main segments of eastward dipping (30-60º) faults with up to 10 m of reverse displacement and a 7 m high escarpment. Each of the three main segments, Fidnajåkka-Biggevarri (south), Masi-Stuoragurra (central) and Iesjavri-Lævnjasjåkka (north), is composed of several sub-parallel segments which are often located in an en echelon pattern. The postglacial fault segments follow to a large extent older fault zones represented by lithified breccias and contacts of albite diabases (Fig. 3). These intrusions within the Mierujavri-Sværholt fault zone occur as both dykes and sills and are 1815 ± 24 Ma (Krill et al. 1985). They are locally strongly foliated after intrusion. Protomylonites also occur along the MSFZ (e.g. in the Neidagårzi area).

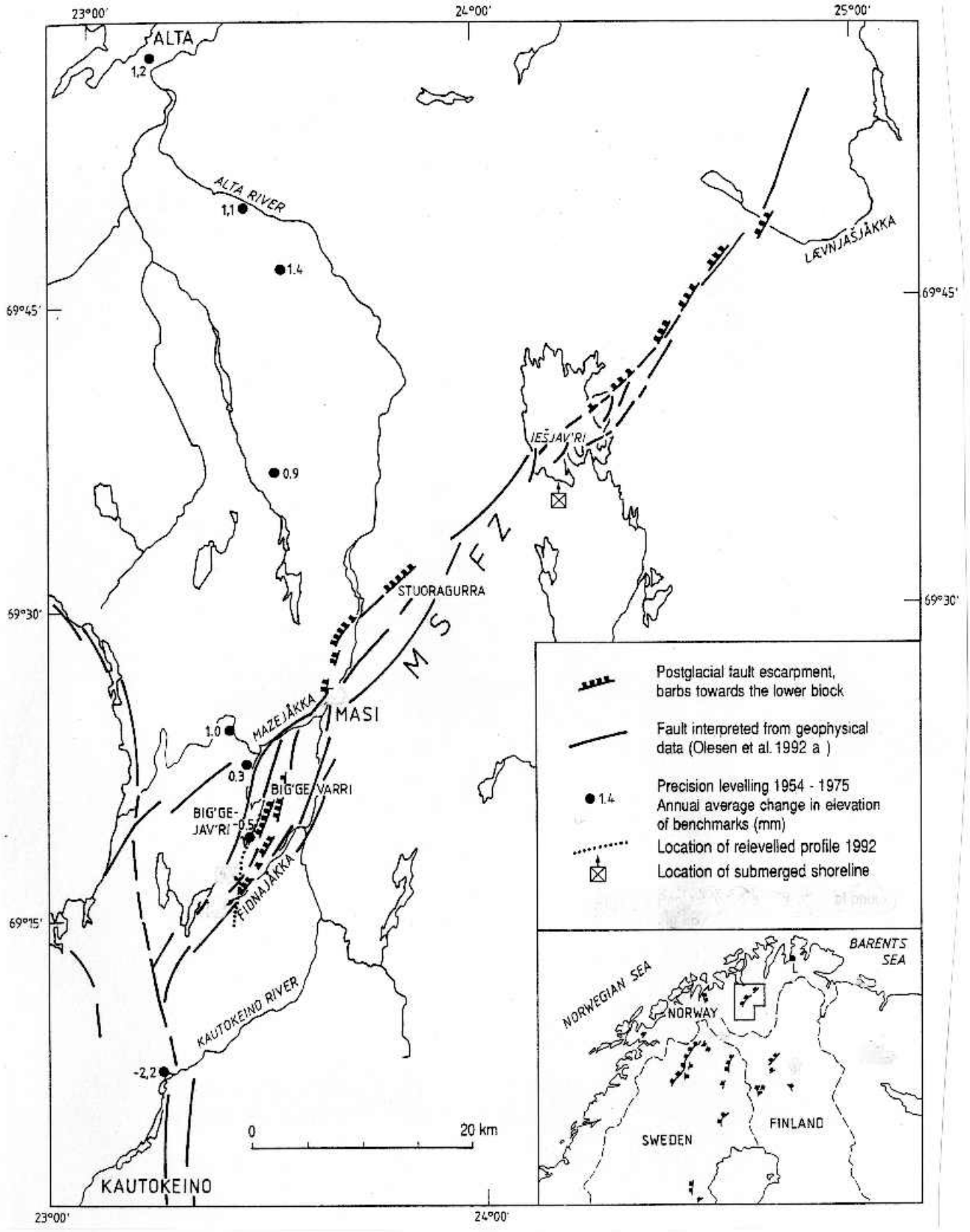

Figure 2. Postglacial faults on Finnmarksvidda. MSFZ — Mierujavri-Sværholt Fault Zone. The annual average change in elevation of benchmarks is based on precision levelling in 1954 and 1975 (Sørensen et al. 1987). Inset map shows Late Quaternary faults in northern Fennoscandia (Olesen 1991). L — offset drillhole locality southwest of Lebesby, Finnmark (Roberts 1991).

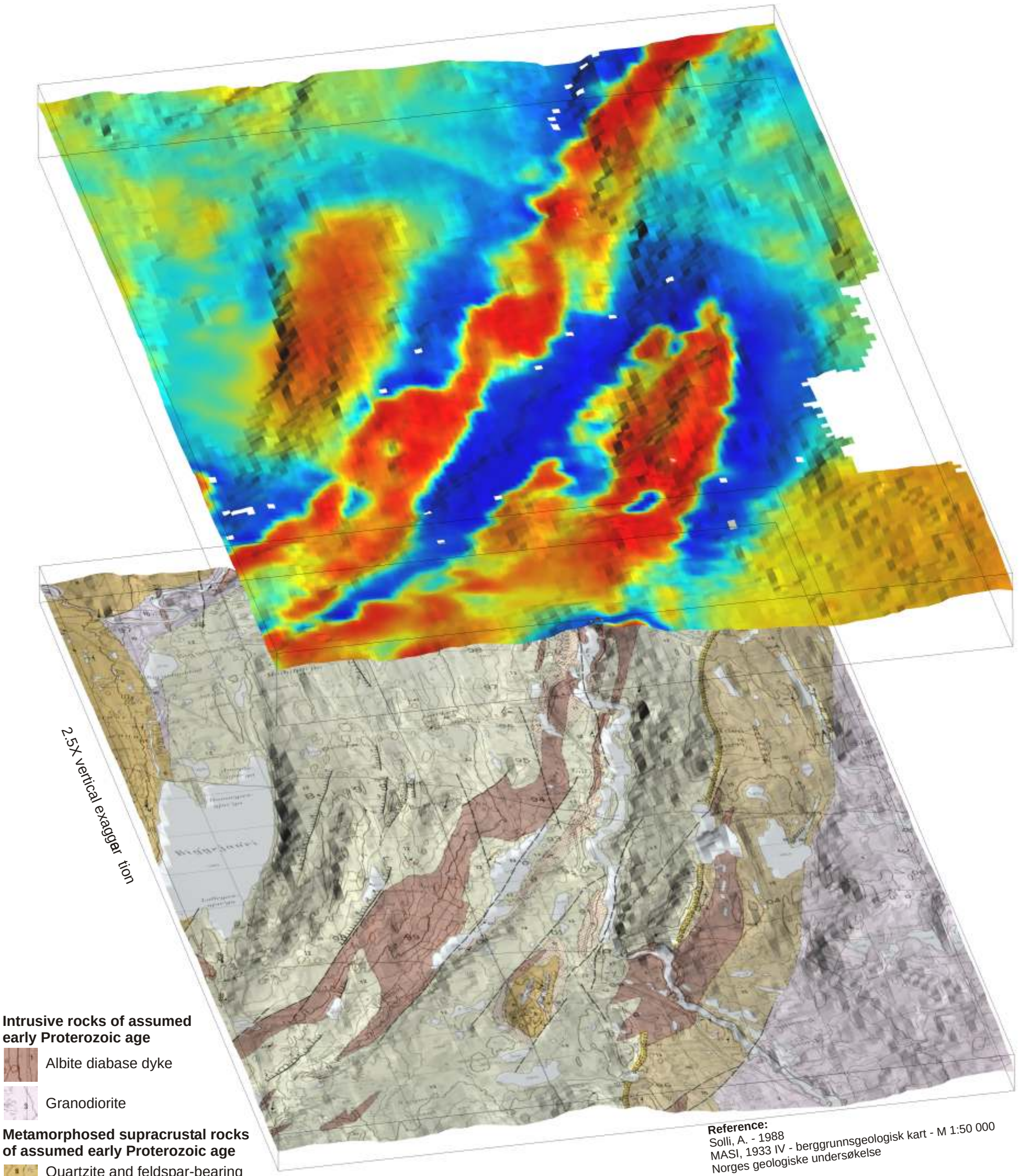

Figure 3. Aeromagnetic map (Olesen and Sandstad 1993) and bedrock geology map (Solli, 1988) from the Skarrejavre-Biggearri area. Magnetic albite diabases occur along the regional Mierujavri-Sværholt Fault Zone. Postglacial faults are reactivated along this fault zone.

The SF cross-cuts glaciofluvial deposits northeast of Iešjav'ri (Olesen 1988) and an esker northeast of Masi (Fig. 4) and is consequently younger than 9.300 years (Olesen et al. 1992a). The postglacial fault coincides locally with an 5-10 m wide zone of lithified breccia and is composed of several thin (a few cm wide) zones of fault gouge within a couple of metres wide zone. The southernmost segment of the fault is listric with a dip of ~ 50° close to the surface and ~ 30° at a depth of more than 40 m. The fault typically has an offset/length ratio of approximately 1/10.000 which is one of the criteria generally applied for the classification of neotectonic faults.

Figure 4. (previous page) Oblique aerial photographs of the Stuoragurra Fault cutting through an esker (UTM 611400-7717300) in Stuoragurra, 12 km NNE of Masi and 1 km south of Savustanjavri. The fault was consequently formed after the deglaciation at approximately 9300 BP. a) Photograph from August 1989; looking SE. The fault scarp is shown by the two large arrows and the intersection with the esker is marked with a small arrow. b) Photograph from January 1996; looking south. The intersection between the fault scarp and the esker is shown by the arrow.

Earthquakes occur in a 20-30 km wide cluster to the southeast of the Stuoragurra Fault (Olesen 1988, Bungum & Lindholm 1997). This spatial correlation has been interpreted by Bungum & Lindholm (1997) to reflect a broad zone of weakness that is responding to the present day stress field. Focal mechanism solutions (Fig. 5b) are consistent with reverse faulting with a dip to the southeast (Bungum & Lindholm 1997).

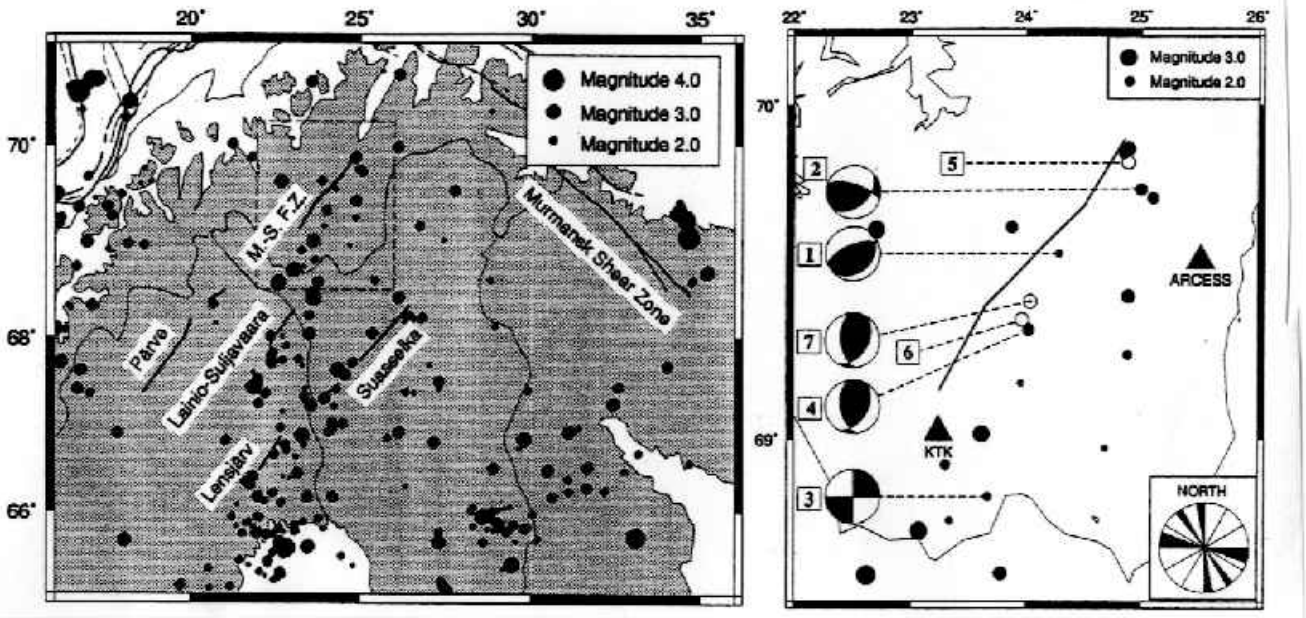

Figure 5. a) Earthquakes from 1979-1992 and postglacial faults (Bungum & Lindholm 1997). b) Focal mechanisms (Bungum & Lindholm 1997) calculated for five earthquakes and earthquakes from 1979-1992 along the Stuoragurra postglacial fault. The trend of horizontal compression as indicated by the fault plane solutions is seen in the rose diagram in the lower-right corner. Earthquake No. 7 represents the magnitude 4.0 earthquake on 21 January 1996.

Several groundwater springs occur along the Stuoragurra Fault. Previous drilling through the fault has revealed high ground water yield (Fig 6). Large amounts of water poured out of the escarpment some time between the 21 January 1996 earthquake (magnitude 4.0) and August of that year (Olesen & Dehls 1998). The Norwegian Water Resources and Energy Administration (NVE) has provided river flow data (Fig. 7) for the period 1989-1997 from the Iesjåkka River, which is draining the area where the M. 4 earthquake occurred. The gauge is located in Jergul, 20 km to the west of Karasjok (Fig. 18). The water level was reduced by 15-20 % during the first weeks after the earthquake and stayed low during the months of February, March and April (Fig. 7) till the snow melting started in the middle of May. These data are, however, hampered with uncertainties since they are not corrected for

changing ice conditions during the winter. Reduced water flow after large reverse fault earthquakes has also been reported from Alaska and Japan (Muir Wood & King 1993). Normal fault earthquakes, on the other hand, cause increased water flow. The fault plane mechanism from the 1996 earthquake shows that it is a reverse fault earthquake (Bungum & Lindholm 1996). Several magnitude 7-8 earthquakes were associated with the formation of the postglacial faults within the Lapland Province (Table 1). If such large earthquakes occurred after each of the numerous glaciations during the Pleistocene, and if the seismic pumping models by Sibson (1981) and Muir Wood & King (1993) are valid, this may have implications for both the occurrence of ground water on land and hydrocarbons offshore.

Figure 6. Percussion drilling through the Stuoragurra Fault in the Skarrejavri-Fidnajåkka area showed high content of groundwater in the fault zone. The yield was estimated to minimum 17 m^3/hour (Klemetsrud & Hilmo 1999) which was the capacity of the most powerful pump available for a 5.5" diameter well. This borehole yield is among the highest ever measured in hard rock aquifers in Norway. The well on the picture is emptied by blowing pressured air into it.

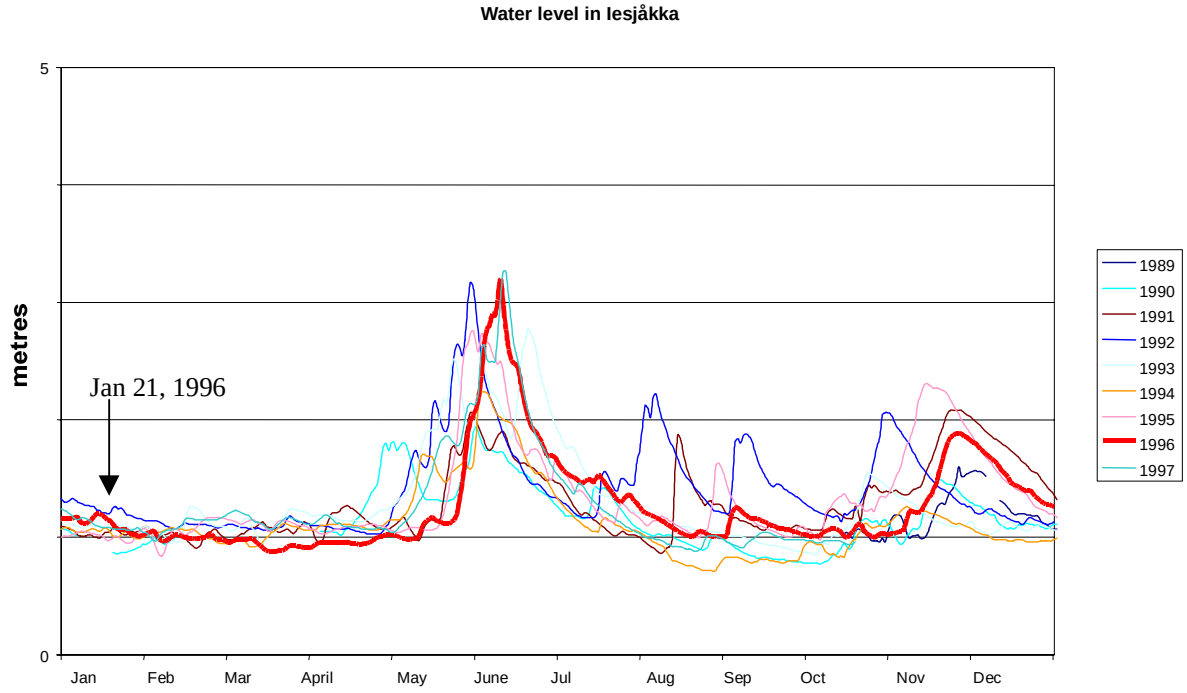

Figure 7. Measured water level at gauge in Jergul, 20 km to the west of Karasjok. The data represents raw data and are provided by the Norwegian Water Resources and Energy Administration, NVE (R. Sværd pers. comm. 1998). The data are not corrected for changing ice conditions during the winter. The water level was reduced by 15-20 % during the first weeks after the earthquake and stayed low during the months of February, March and April.

Precision levelling of benchmarks across the Stuoragurra fault has shown that the footwall block has subsided relative to the hanging-wall block by 2.3 mm between 1987 and 1991. This displacement is statistically significant at a level higher than 95%. The annual average change in elevation of benchmarks based on precision levelling in 1954, and later in 1975 along the old road from Alta to Kautokeino, has shown a significant deviation from the general postglacial upheaval of Fennoscandia. Instead of an increasing uplift from 2 mm/year in Alta to 5 mm/year in Kautokeino, as is generally indicated on land upheaval maps of Fennoscandia, a subsidence of the inland area was observed. During Quaternary geological mapping in the Iešjav'ri area one submerged shoreline has been observed at the southern margin of this lake. The shoreline is located roughly a few dm below the present water-level, and we think that this indicates that a vertical crustal movement with a N-S gradient opposite to that of the general postglacial rebound has occurred during the last few hundred years. Relevelling of the profile of 1954 and 1975 by the Norwegian Mapping Authority (SK) did not, however, reproduce this pattern (Olesen et al. 1992c).

It is unclear if the present seismicity implies that the faults are still active and represents a seismic hazard. Trenching of the Stuoragurra Fault in 1998 (Olsen et al. 1999) revealed that the fault scarp is formed during one major event shortly after the deglaciation of the area (Fig. 23). This in concert with the conclusions by Lagerbäck (1990) for the Lansjärv postglacial fault in northern Sweden.

Several questions arise after the recognition of the Lapland province of postglacial faults. Did similar postglacial faulting occur after each of the several glaciations during the Pliocene and Pleistocene? Did postglacial faulting occur in the mountainous parts of Nordland and western

Norway which are seismically more active than the Lapland area but where this type of faulting is more difficult to recognise?

Studies of the postglacial Stuoragurra Fault in the Precambrian of Finnmark showed that postglacial faulting is likely to occur in areas of increased seismicity, regional zones of weakness and anomalous land uplift (Olesen et al. 1992a,b).

1.2 The Nordmannvikdalen Fault

The Nordmannvikdalen postglacial fault (Fig. 8), which was discovered by Tolgensbakk & Solli (1988), is a normal fault dipping 30-50° to the northeast. The height of the escarpment is up to 1 metre (Figs. 9 & 10). The fault is locally anastamosing, branching out in 2-3 sub-parallel faults (Fig. 10). Sollid and Tolgensbakk (1988) suggested that the abundant rock avalanches in the area are formed during this postglacial faulting.

The fault is situated along the gradients of parallel gravity and magnetic anomalies that are interpreted to represent structures in the underlying Proterozoic basement, which is situated at a depth of ~ 3 km in this area (Olesen et al. 1990). The fault does also coincide with a NNW-SSE trending gradient in the depth to the Precambrian basement surface, which increases from a depth of 1-2 km in the Reisa area to more than 3 km in the Lyngen area to the west (Map Enclosure 3).

Figure 8. The Nordmannvikdalen postglacial fault seen from the northwest.

Ground penetrating radar (GPR) profiles at Nordmannvikdalen were carried out within the NEONOR Project to try to determine whether the Nordmannvikdalen fault is a gravitationally induced fault or a true tectonic postglacial fault (Mauring et al. 1997, Mauring et al. 1999). Varnes et al. (1989) suggest that gravity induced sliding is most likely to occur when the

elevation difference is greater than 300 m. At Kåfjord, the slope of the terrain is 10-12º, and the elevation difference between the fault scarp and the valley bottom is 150-200 m. Thus, gravitational sliding seems less likely, but still has to be considered.

If the scarp in Nordmannsvikdalen represented the head of a gravitational slump feature, we would expect to see several phenomena. First, the scarp should be somewhat arcuate in shape. This is not the case. The curvature seen in map view is due to the topography (see below). Second, we should see some sort of accommodation structures along the sides. The western end of the scarp terminates against a large rock flow. Due to the large size of the blocks, it is impossible to determine the relative ages of the two features. It is possible that the rock flow conceals the original side of a slump, however, there is no evidence pointing towards this. The eastern end of the scarp terminates against the edge of a mountain (Fig. 9). Here, there is clearly no evidence for slumping. Third, we should see the foot of the slump along the valley floor. Although there are numerous small terraces between the scarp and the valley floor, there is no feature that could be interpreted as the toe of a slump (Fig. 8).

Figure 9. The easternmost end of the Nordmannvikdalen fault terminates against the side of a mountain. The rubbly nature of the mountain side makes it difficult to determine if the fault continues, and if so, in which direction.

The GPR records show that the feature is a surface expression of a structure dipping 40-50° towards the north-east. An abrupt offset in the terrain surface corresponds with the position of the up-dip extrapolation of the most prominent radar reflector. This could indicate that the dipping reflector represents a structure that has been active during Holocene (i.e. postglacial activation). A relatively constant dip of the structure towards the north-east on two profiles indicates tectonic faulting. A third profile shows, however, a gentler dip of the structure towards depth, which is in favour of a gravitational induced faulting.

The fault scarp in Nordmannvikdalen runs over two gentle hills and is cut by two stream beds. It was thought that a digital elevation model (DEM) would allow us to estimate the dip of the fault by standard geometrical techniques. A DEM, and accompanying orthophoto, were produced by Fjellanger Widerøe A/S (Fig. 11). One metre elevation contours were supplied in vector format, as well as lake edges, stream paths and cliff edges. A model was built within Arc/Info, which was then used to produce a grid with a one metre cell size.

Figure 10. Photograph of the escarpment of the Nordmannvikdalen postglacial fault looking NW. The picture shows a bifurcation of the fault scarp.

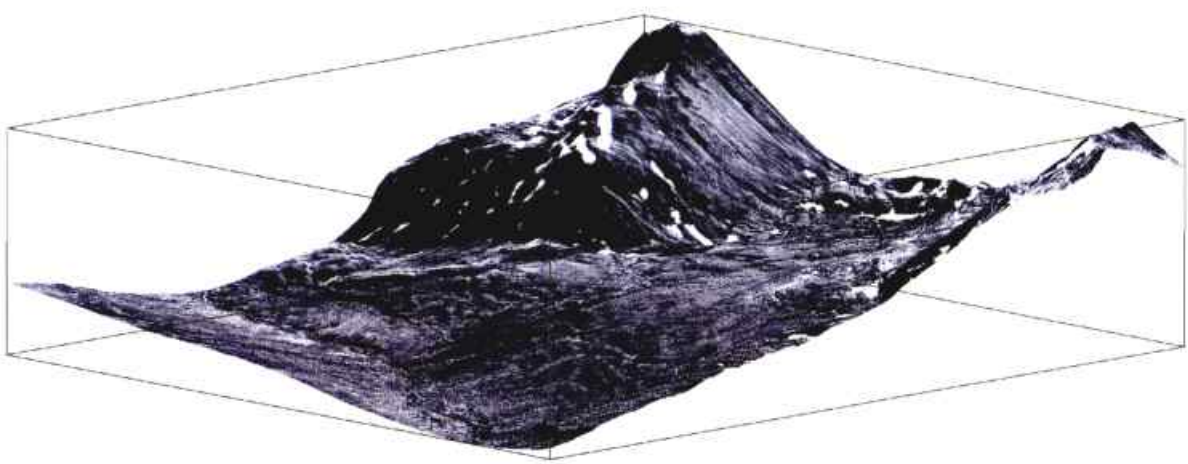

Figure 11. Orthophoto draped over a DEM of the area around the Nordmannsvika fault. View is from the northwest. Sides of the box are 2500 metres.

The traces of both the bottom and the top of the fault scarp were digitized. The x, y, and z values of the DEM along the traces were then used to fit an optimum plane through the points. A least-squares algorithm was used. The resulting plane has a dip of 28º to the northeast (Fig. 12). This is obviously much shallower than the reflectors seen in the GPR. However, this can be explained by the different mechanical properties of the overburden, in which we have done our analysis, and the bedrock. If the overburden is lying upon a planar bedrock surface, and the local relief is due to variations in overburden thickness, then this 3D analysis only reflects the orientation of the dip within that overburden. The fault plane cannot continue upwards through the overburden at the same steep angle at which it cuts the bedrock, and thus the analysis does not contradict the results of the GPR studies. However, if the surface relief reflects the bedrock relief, and there is a layer of overburden with constant thickness, then this argument cannot be applied, and we must find another explanation for the apparent contradiction.

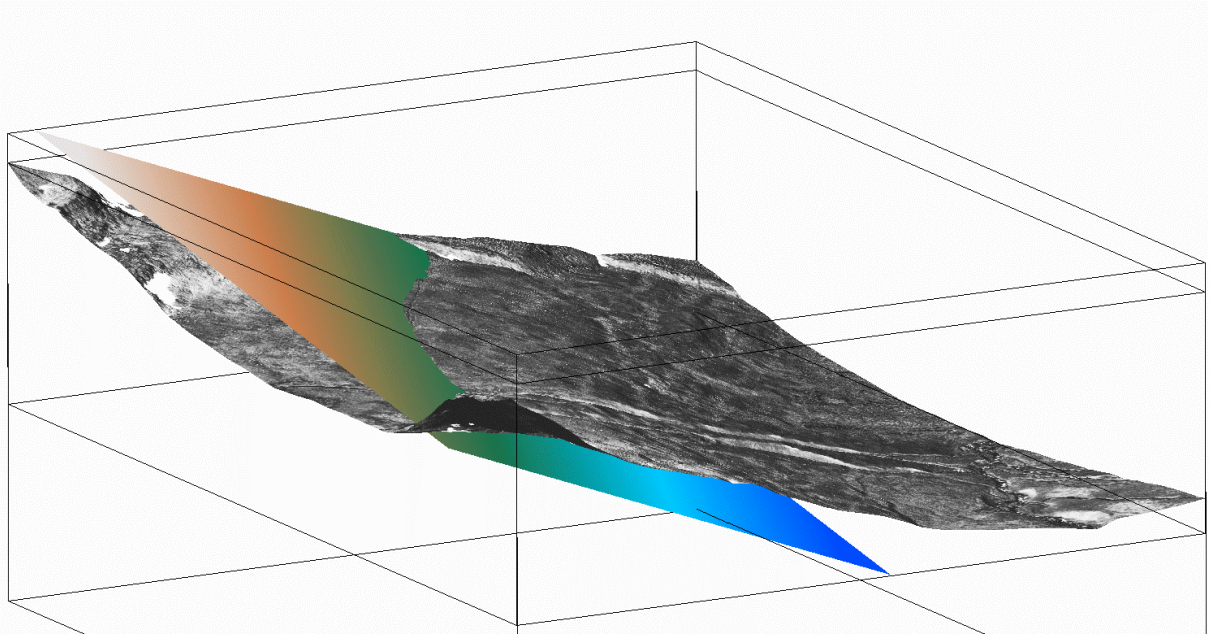

Figure 12. The best-fit plane through the trace of the fault scarp dips 28º to the northeast. View is from the southeast.

Hovland & Judd (1988) reported the occurrence of several pockmarks at the sea floor in the Lyngenfjord. Two of the locations are situated along the NW extension of the Nordmannvikdalen postglacial fault and the nearest pockmark is located only 5-6 km from the fault. The pockmarks have been attributed to either groundwater from a hydraulic head caused by nearby high mountains with lakes, streams and glaciers, or to substantial volumes of biogenic gas generated by the decomposition of organic matter in the fjord sediments. It is possible that an earthquake associated with the formation of the postglacial Nordmannvikdalen fault has triggered the release of groundwater or gas.

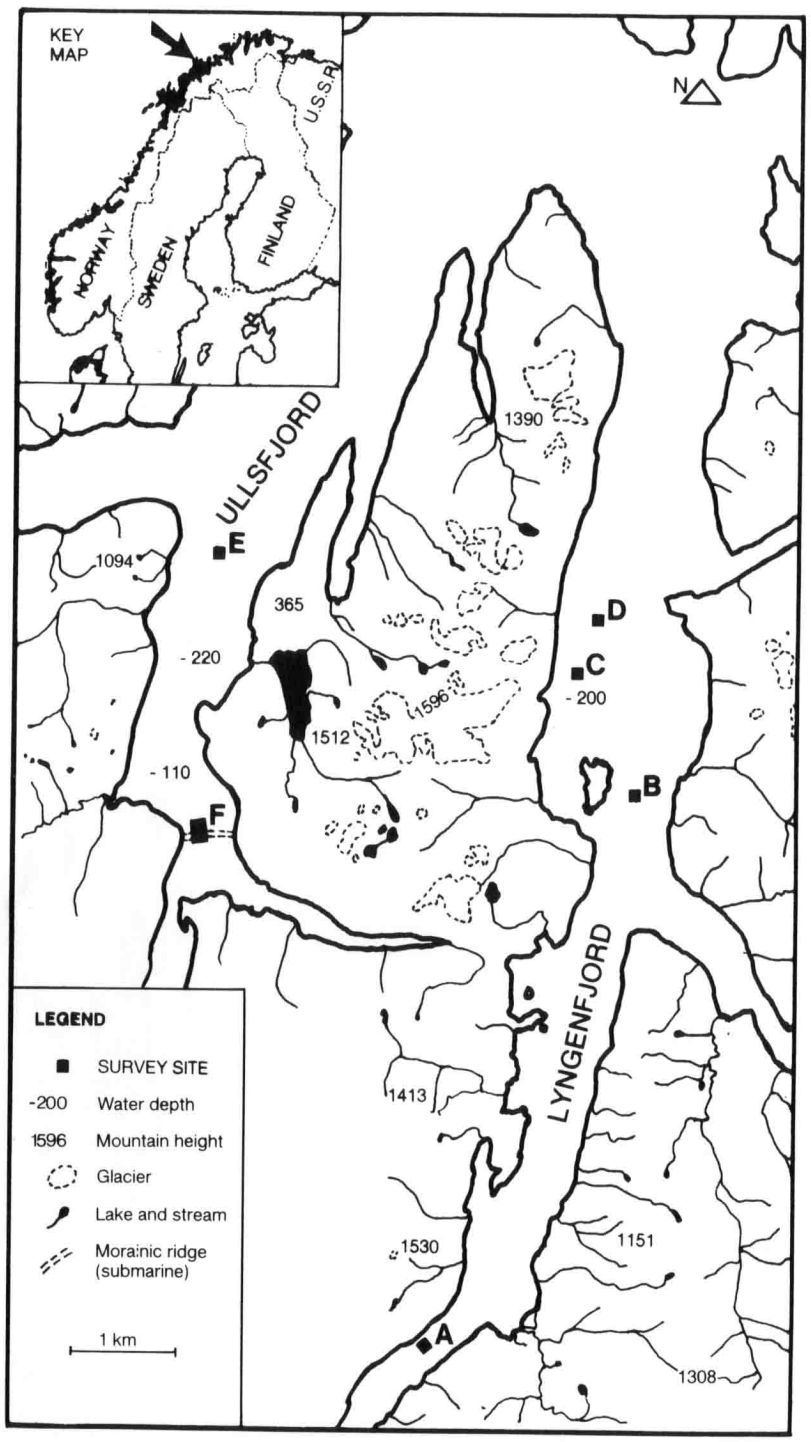

Figure 13. Locations of pockmarks (location A, B and D) and doming of the seabed (location C and E) in Lyngenfjorden and Ullsfjorden (Hovland & Judd 1988). Nordmannvikdalen is situated to the east of location B in Lyngenfjorden.

1.3 Rock avalanches and gravitational faulting in Troms county

It is known from studies of the effect of historically known earthquakes that many of them trigger different types of avalanches, including large rock avalanches (e.g. Keefer 1984; Jibson 1994). The history of rock avalanches could thus be used for palaeoseismic analysis, but this requires detailed mapping of their spatial occurrence and dating of individual events. The review made by Jibson (1994) indicates that large rock avalanches require a minimum earthquake magnitude of about 6.0, and he also concluded that large rock avalanches are the type of avalanche with greatest potential in palaeoseismic studies.

Geological studies of rock avalanches in Troms demonstrate a surprisingly high number of events in the Kåfjord and Storfjord areas. Studies from the early seventies also show this pattern (Corner 1972). There are several large-scale gravitational features in this area, characterised by large faults and crevasses. These gravitational features have been observed as far east as Nordreisa where several portions of the eastern mountain slope has slipped down.

We will see several large rock avalanches during the drive from Tromsø to Kåfjord.

Attempts on dating some of the rock-avalanche events have been given priority. Seismic surveys on one avalanche in Sørfjorden, a fjord west of the Lyngen peninsula, indicate that this event occurred shortly after the deglaciation (ca. 10000-9500 years BP). The same conclusion has been made about a rock avalanche studied in Balsfjorden. Three radiocarbon dates on shells that are younger than the avalanche event gave ages between 9500 and 9600 radiocarbon years BP. A large bedrock collapse west of Salangen formed huge blocky rock-avalanche deposits. Road cuts through this avalanche exposed marine sediments with mollusc-shells on relatively high altitudes. Two dates on these shells show that the avalanche was older than 9900 radiocarbon years BP (and older than ca. 10.300 BP). Another rock avalanche further west on Andørja was dated to be older than 9500 radiocarbon years BP. The preliminary conclusions of this study indicate that the rock avalanches in Troms are concentrated to specific zones, and they seem to be old, formed shortly after the deglaciation. This might imply that there were major earthquakes in the period 10000 to 9500 years BP and which possibly can be correlated with the postglacial faulting in Nordmannvikdalen.

2. ITINERARY

2.1 Day 1: Troms county

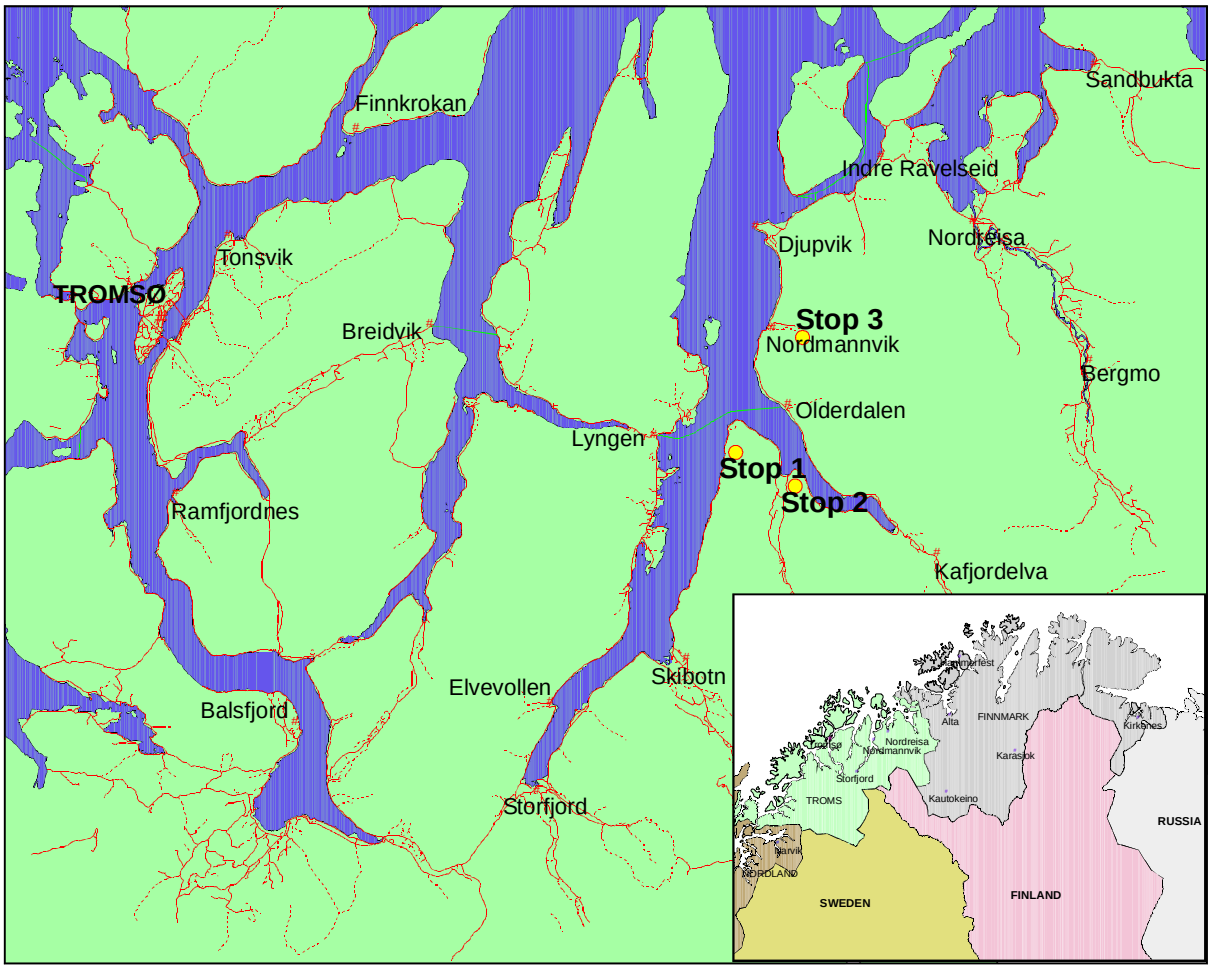

Figure 14. Locations map for Day 1.

2.1.1 Location 1 Nordnesfjellan, Map sheet 1634 III Lyngen and 1634 II Kåfjord (UTM 477000, 7716000)

From Tromsø, drive south on E78 to Nordkjosbotn. Continue on E6-E78 north to Olderbakken. Continue northwards on E6 to Nordnes. (Approximately 160 km from Tromsø.)

Major gravitational faulting has been mapped on Nordnesfjellet, north of Skibotn (Fig. 15), in an area covering more than 2 km in length. The faults or crevasses are localized on a quite flat plateau and extends up to 400 m from the mountain slope. The most striking observation is that there seems to be a more or less horizontal displacement along the foliation planes. Horizontal displacements of as much as 10 m have been observed here. One of the faults seems to be covered by a small lobate feature that has been interpreted to be a small rock glacier.

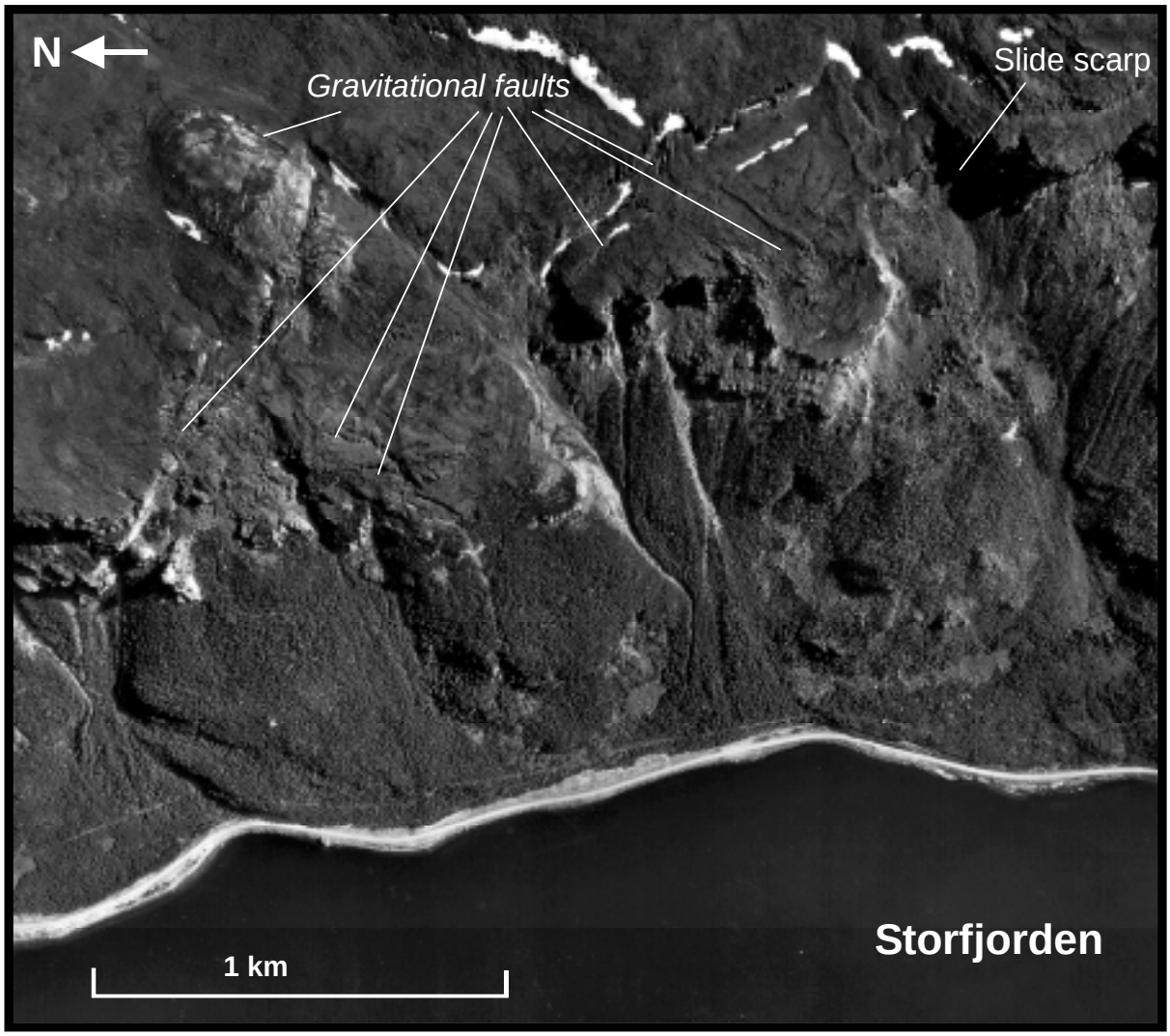

Figure 15. Gravitational faults on top of Nordnesfjellet, north of Skibotn in Troms.

2.1.2 Location 2, Manndalen, Map sheet 1634 II Kåfjord (UTM 483000, 7714000)

Continue aproximately 10 km to Manndalen.

Fig. 16 shows one large gravitational fault in Manndalen. Parts of the fault scarp is also here covered by a lobate feature. We need to go back to the Younger Dryas period (11,000 – 10,000 radiocarbon years before present) to find a climate which is cold enough to get active rock glaciers. A part of the gravitational faulting is thus interpreted to have started before 11,000 BP. The size and the large horizontal displacement might indicate that large-scale earthquakes are the most probable triggering mechanism.

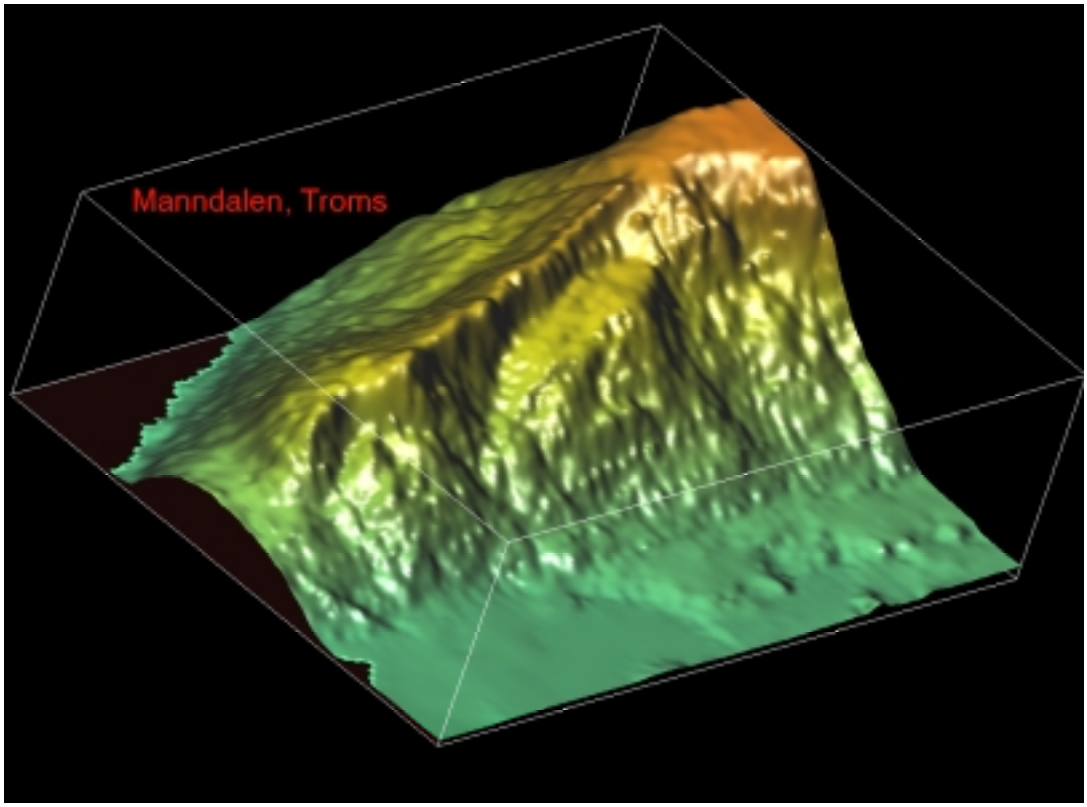

Figure 16. DEM from Manndalen showing a gravitational slide.

2.1.3 Location 3, Nordmannvikdalen, Map sheet 1634 II Kåfjord (UTM 486000, 7726000)

Continue approximately 40 km along E6 to Nordmannvik. Turn right on the first gravel road south of town, just before the bridge over Vikelva. Drive 3 km, park and walk 4 km through the valley of Nordmannvikdalen and up to the postglacial fault on the southern side of the valley (below Skavlekila and Nordmannviktinden).

There is a very high number of large rock avalanches close to the Nordmannvikdalen postglacial fault. One of them is situated almost in directly contact with the fault (Fig. 17). Mapping of a large rock avalanche at the fjord north of Nordmannvika evidenced marine abrasion and formation of beach terraces on high altitudes, demonstrating that the event occurred shortly after the deglaciation.

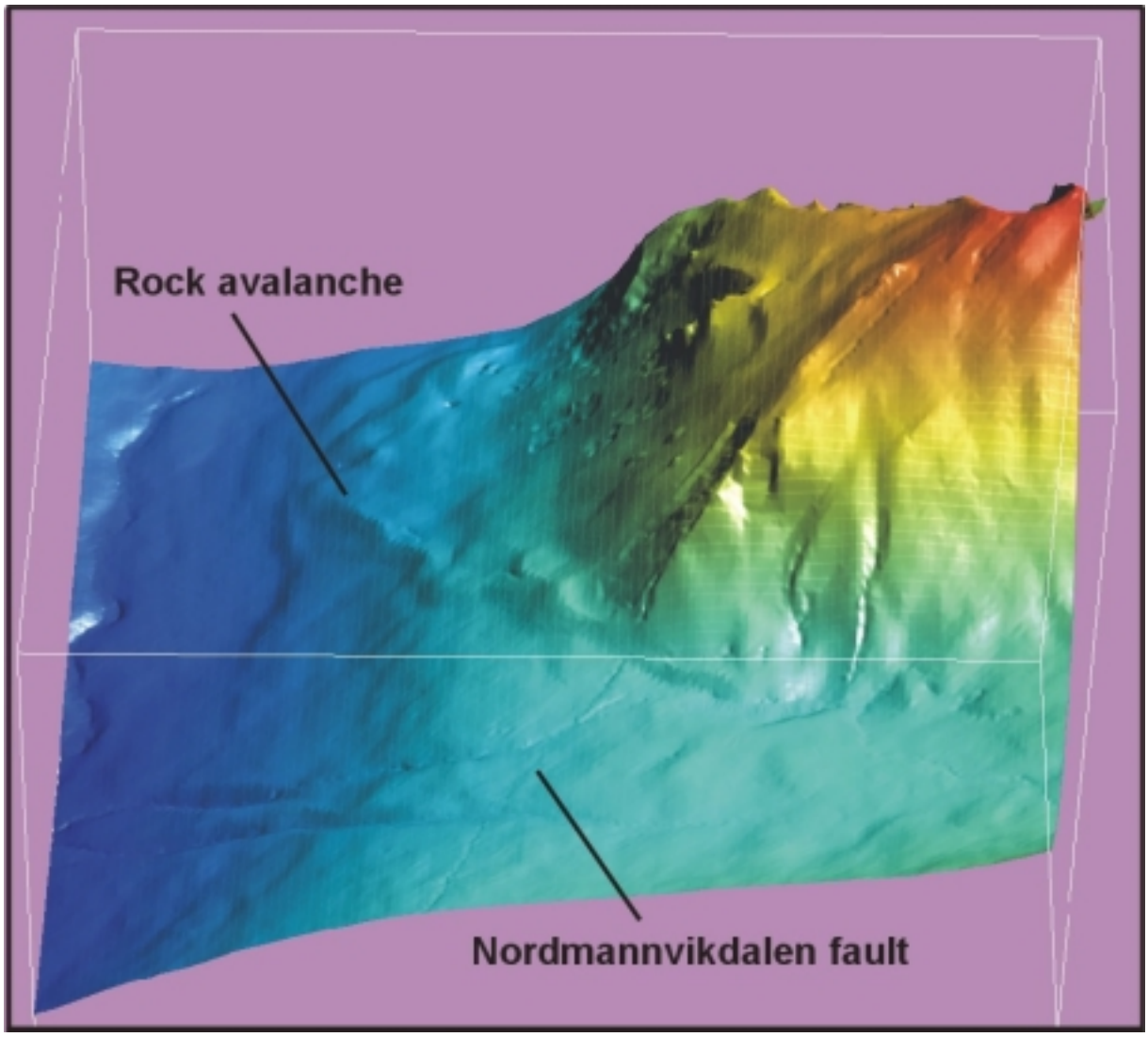

Figure 17. DEM of a large rock avalanche close to the Nordmannvikdalen postglacial fault. View is from the northwest.

2.2 Day 2: Stuoragurra Fault, Masi, Finnmark county

See Fig. 18 for stop locations.

2.2.1 Location 4, Skarrejavri–Fidnajåkka, Map sheet 1933 IV Masi, (UTM 596200-7687000)

Drive 210 km north from Nordmannvik to Alta.

Drive 115 km from Alta to Mierujavri (Mieron) and turn right one kilometre before the village. Drive ~18 km northwards along the old road in the direction of Masi. Stop 200 m to the north of Skarrejavri (Figs. 18-20). Walk for 200 m in NE direction to find the southernmost part of the Stuoragurra Fault. Continue for 500 m along the escarpment to the westernmost shore of a small lake where the fault steps over to the east to follow the easternmost shore of the lake. This geometry opens up the possibility for a possible dextral strike-slip component along the Stuoragurra Fault causing subsidence and formation of a sag

pond along the fault. East-west trending depressions are located to the southwest of the lake. These structures most likely represent secondary extensional structures formed between the two faults. A spring occurs approximately 300 metres to the south of the small lake and 20 metres to the west of the escarpment. Nothing but the flower *Viscaria Alpina* and some moss grow in a 25 m long and 3-5 m wide field downstream from the spring revealing that the ground water has a quite high content of heavy metals. Chemical analysis of three soil samples shows copper contents of 0.36, 0.50 and 1.34%. Induced polarisation (IP) measurements in the area show, however, that the sulphide content in the bedrock along the fault is very low.

This part of the Stuoragurra Fault has been studied with a variety of geophysical methods in addition to percussion and core drilling. The fault surface is composed of several thin (a few cm wide) zones of fault gouge within a 1.5 metre wide zone. The fault gouges have sealing properties. Ground water was encountered in BH4 at a depth of 35 m (2 m above the main fault zone). After penetration of the fault gouges at a depth of 37 m, the ground water was drained but appeared again at a depth of 40 m. The fault gouges did consequently cause a 'hanging' ground water surface above the main fault zone. Lithified fault breccias (Fig. 22) also reveal that an older zone of weakness has been reactivated. The location of the main fault zones from the core drilling (Fig. 21) is consistent with the results from the geophysical measurements (Olesen et al. 1992a, Roberts et al. 1997).

A listric shape of the fault has been inferred from the combined data sets. The dip of the fault is 55º close to the bedrock surface (Olsen et al. 1999) and 35º between drillholes 4 and 7 (see Fig. 21). Interpretation of the aeromagnetic data shows that the dip of the albite diabases in the Fidnajåkka area is 40º to the SE (Olesen 1991). The results from the drilling may indicate that the postglacial fault merges with the fault zone below the albite diabase.

During 1998, two trenches were made across the Stuoragurra Fault, between Kautokeino and Masi (Olsen et al. 1999). For the first time, the fault was directly observed in the bedrock. The hanging wall was seen to be thrust upwards over the footwall, with 7 metres vertical displacement evident from displaced glacial contacts (ablation material, including glaciofluvial sediments, overlying lodgement till). The fault did not penetrate the overlying glacial materials, but rather folded them, forming a blind thrust (Fig. 23). Large liquefaction and other deformation structures were found in the glaciofluvial sediments in both trenches. Veins of angular and subangular pebbles from the local bedrock (Masi Quartzite) penetrate more than 10 metres laterally from the thrust plane and into the sediments in the footwall. It is thought that these veins were possibly injected during the fault activity (Olsen et al. 1999). The major deformation of the sediments has a décollement plane that continues laterally in the E/B horizon contact of the modern soil on top of the footwall. This may indicate that an initial pedogenesis had taken place before the fault activity occurred, however no macro plant fossils to support this were found in the possible buried soil. Deformational structures seen in the trench can be explained as a result of one major fault event.

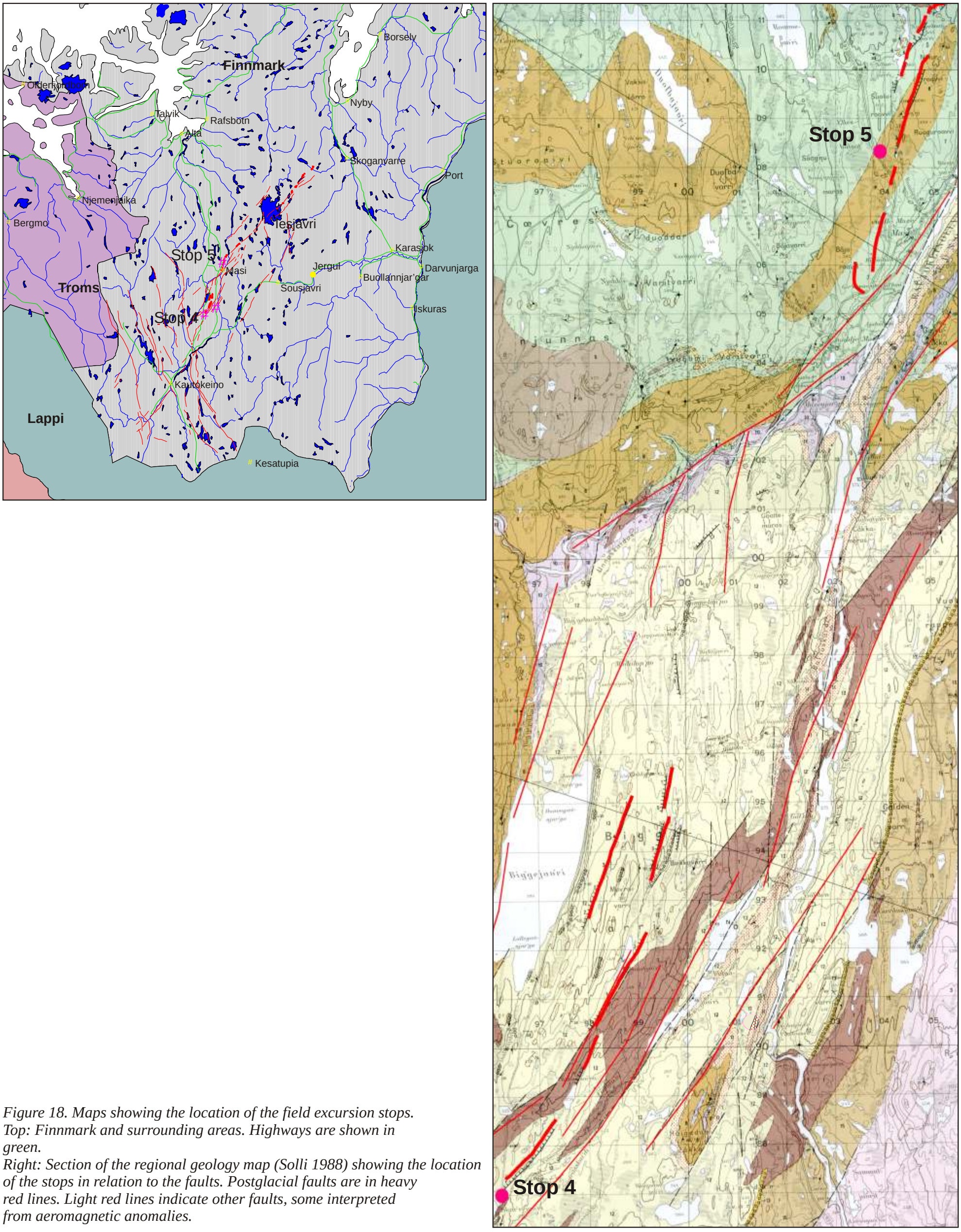

Figure 18. Maps showing the location of the field excursion stops. Top: Finnmark and surrounding areas. Highways are shown in green.
Right: Section of the regional geology map (Solli 1988) showing the location of the stops in relation to the faults. Postglacial faults are in heavy red lines. Light red lines indicate other faults, some interpreted from aeromagnetic anomalies.

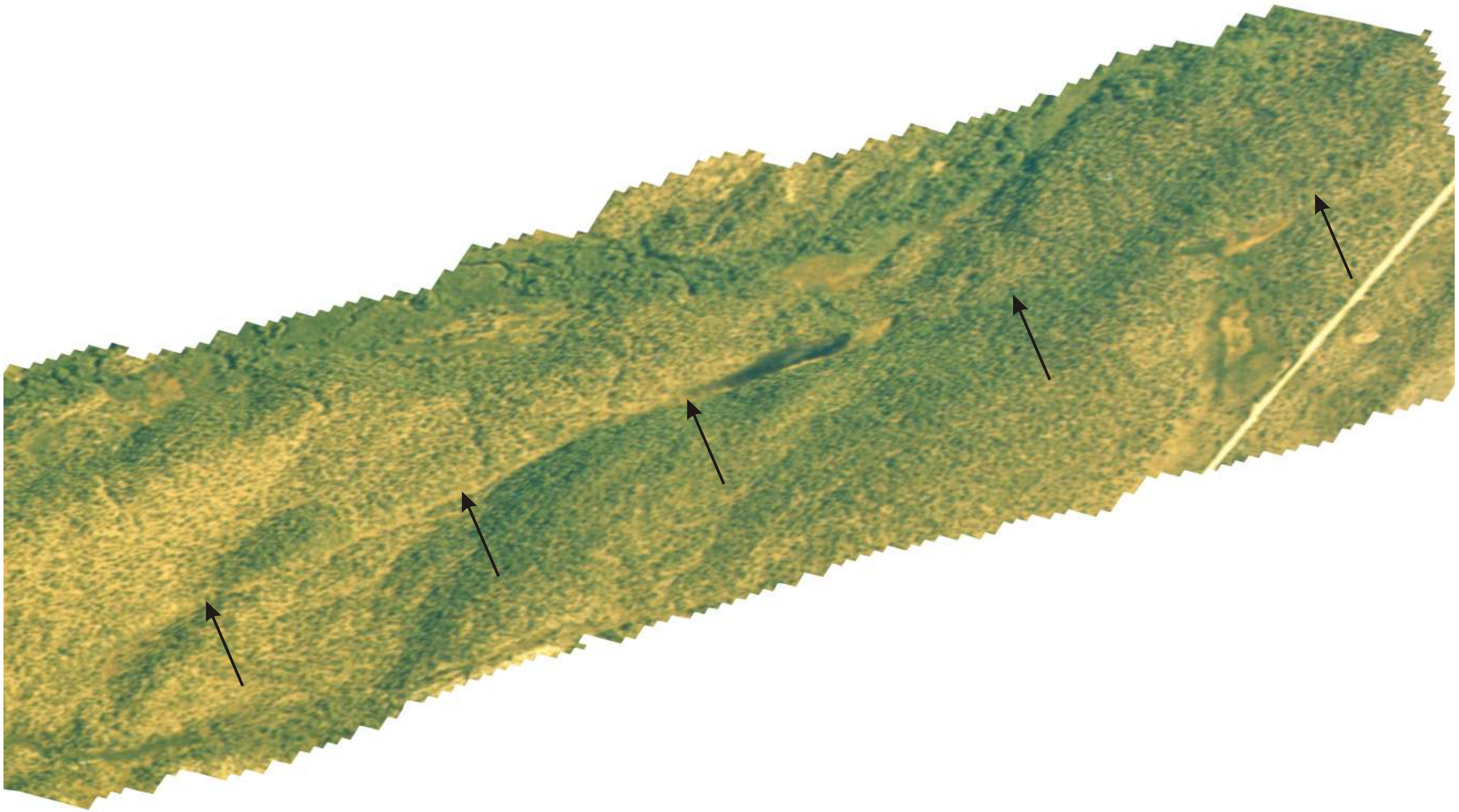

Figure 19. Aerial photograph of the Skarrejavri-Fidnajåkka area (Location 4) draped on a digital terrain model. The fault is shown by the arrows. The view is to the SE and covers the same part of the Stuoragurra Fault as Fig. 10. Part of the old road between Kautokeino and Masi can be seen to the west.

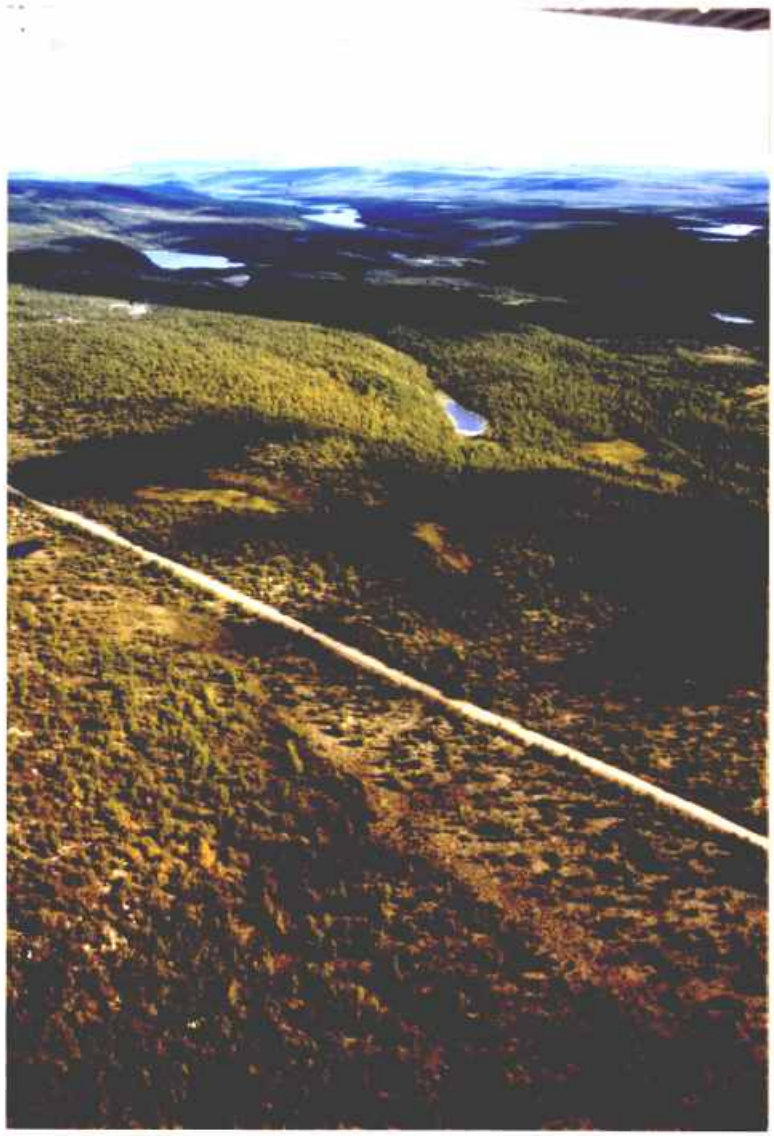

Fig. 20. Oblique aerial photograph of the Stuoragurra postglacial fault to the north of Skarrejavri looking NE (Location 4). The location is shown in Fig. 18. The SF starts immediately to the north of the road (where cars can be parked) and continues down to the lake where it steps from the left-hand side to the right-hand side of the lake. It continues further across an upheaval (UTM 597000-7688000) in the terrain where drilling and extensive geophysical investigations have been carried out (indicated by the large arrow). This locality was also chosen for percussion drilling and test-pumping of ground water yield in August 1998. Further to the north the escarpment can be traced on the northern side of a lake. Precision levelling is carried out along the road in the foreground. The small arrows shows approximate locations of GPS bench marks.

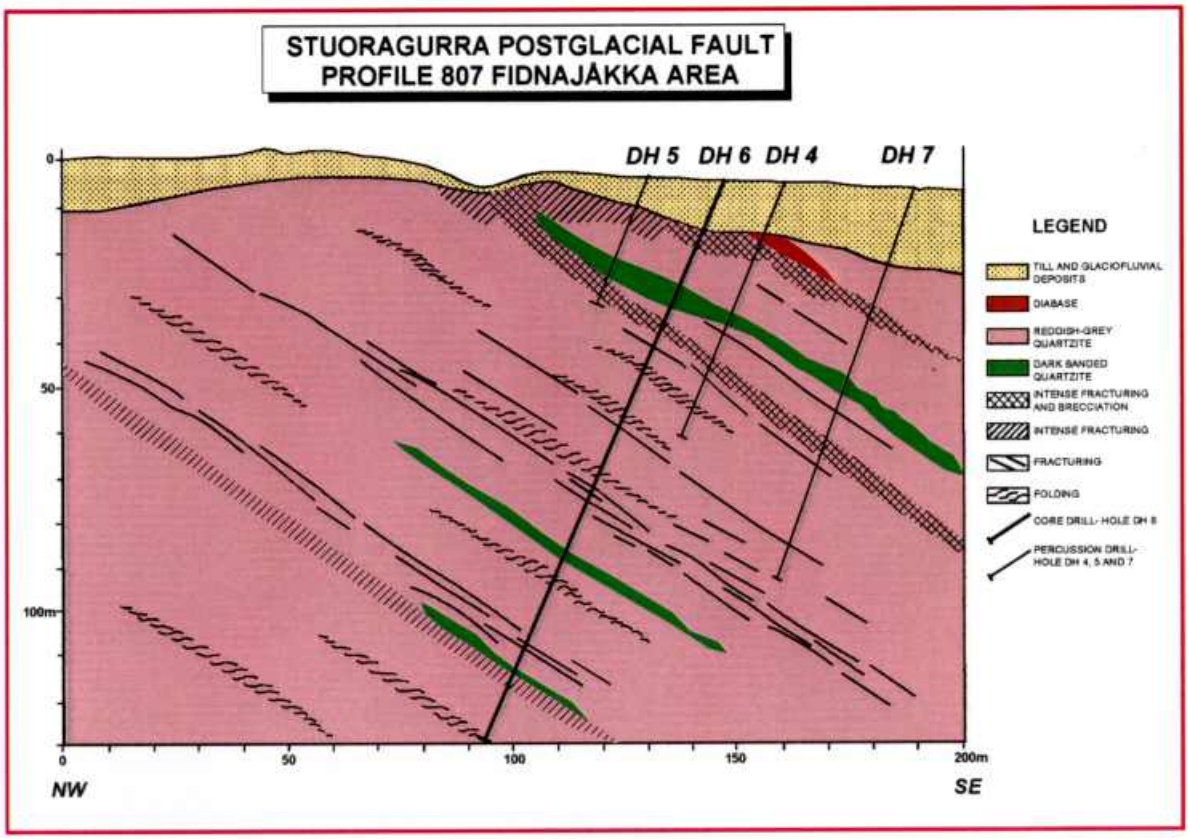

Fig. 21. Interpretation of Profile 807 based on core-drilling, percussion drilling and geophysical measurements (Modified from Olesen et al. 1992a, Roberts et al. 1997).

Figure 22. Photograph of polished sample from the brecciated reddish-grey quartzite from the escarpment.

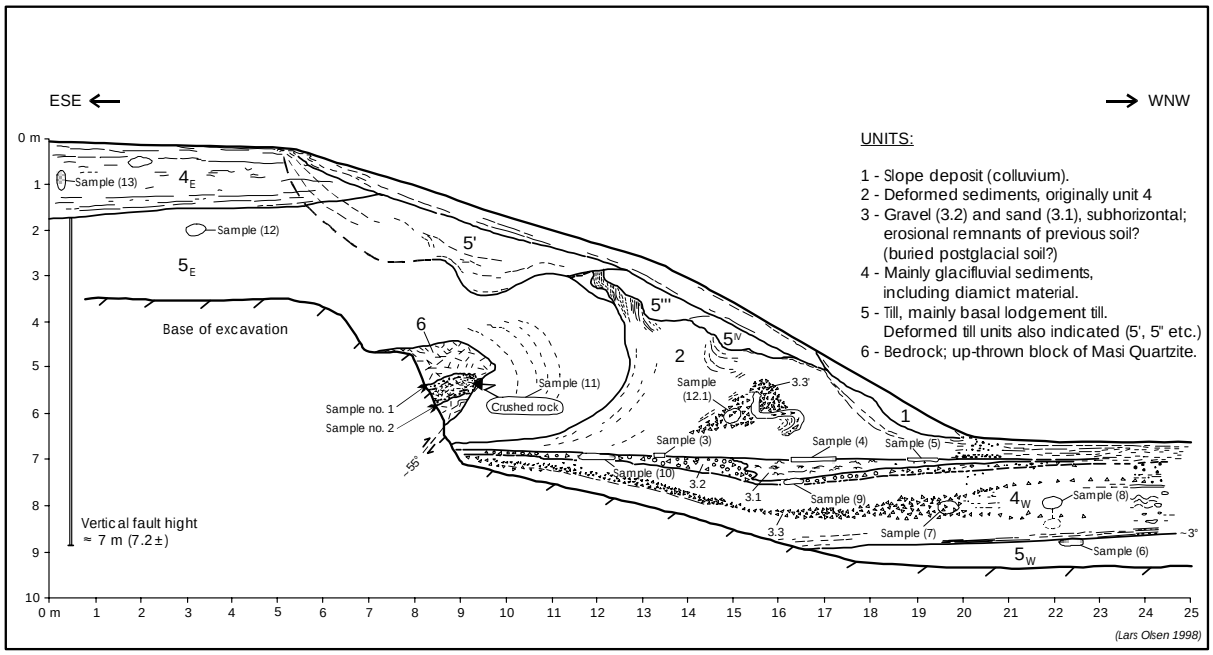

Figure 23. Outline of the northernmost trench at Fidnajohka. The orientation of the section is normal to the fault. The nose of the up-thrown block of bedrock (6) is buried by deformed basal till (5E) and glaciofluvial gravel and sand (2, 3 & 4), with colluvial slope deposits (1) on top.

Levelling of benchmarks in outcrops and large boulders along the old road from Mierujavri (Mieron) to Masijåkka in 1954 and 1975 by the Norwegian Mapping Authority (SK) showed significant deviations from the general postglacial upheaval of Fennoscandia. Instead of an increasing uplift from 3 mm/year at Masijåkka and 4 mm in Mierujavri as is generally indicated on land upheaval maps of Norway, a subsidence of the inland area was observed. A gradual decrease from 1 mm/year at Masijåkka to -2.2 in Mierujavri (Mieron) was observed (Fig. 24). Relevelling of part of this line in 1992 did not, however, reproduce this pattern. A vertical displacement of 3.4 mm was observed between two of the benchmarks lying on either side of a 3 km long southward extrapolation of a fault scarp on Biggevarri. These observations may be related to either:

1) A systematic error in the measurements from 1954.

2) Varying deformation with time and space.

A systematic error in the measurements, which could have caused the observed consistent pattern of subsidence, is unlikely since the profile was levelled in both directions.

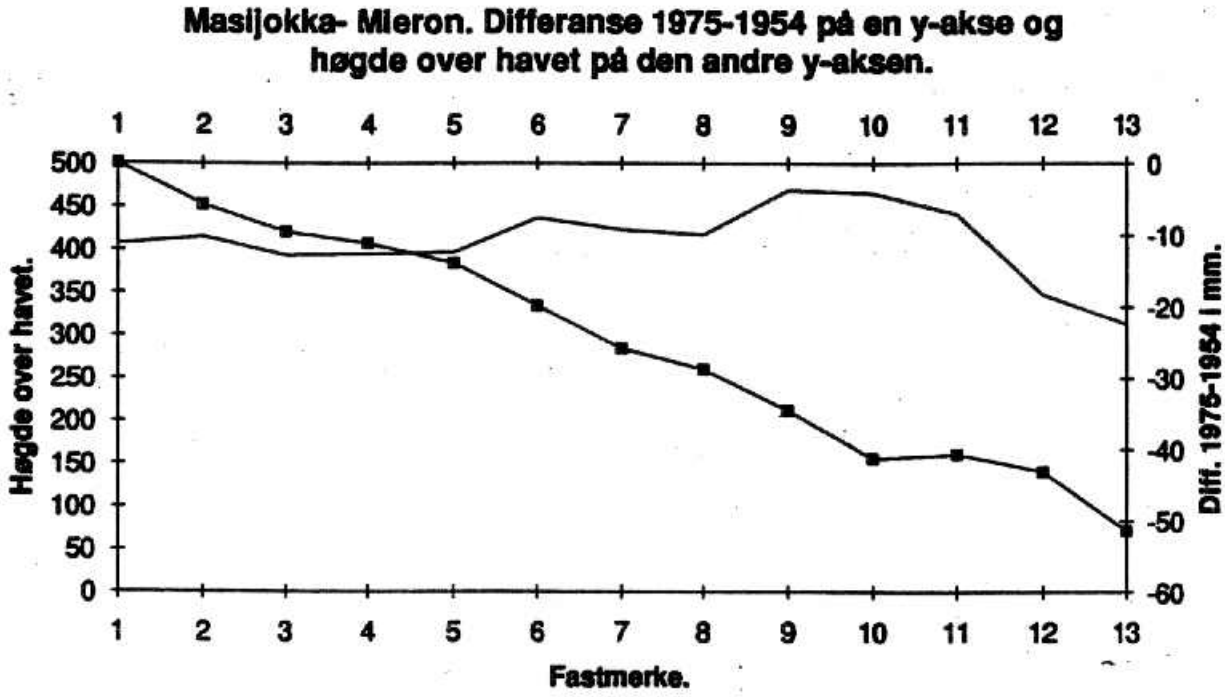

Fig. 24. Difference in elevation (filled squares) along relevelled profile in 1975 relative to levelling in 1954 (Skjøthaug, pers. comm., 1992; Olesen et al., 1992c). The profile is located along the old road between Masijåkka and Mierujavri (Mieron). The uplift decreases to the south, which is opposite to the regional trend.

2.2.2 Location 5, Masi, Map sheet 1933 IV Masi, (UTM 603800-7708300)

Drive back 18 km southwards along the old road to Mierujavri. Drive 46 km northwards along the main road to Masi. Park 2.5 km north of intersection from main road to Masi Church.

Walk 500 m eastwards along tractor track to small lake (UTM 604250-7708250) at the Roavvejåkka stream.

A section of the Stuoragurra postglacial fault continues to the north of the lake for 2 km in a NNE direction. The maximum height of the escarpment is 7 metres in the central part of the fault section. The height decreases gradually to the north and the south from the central part.

Outcrops of brecciated amphibolite occur along the escarpment. The schistosity of the surrounding amphibolite has been mapped utilising measurements of the anisotropy of magnetic susceptibility (AMS) (Olesen et al. 1992b). The strike of the schistosity coincides with the strike of the postglacial fault. The dip of the schistosity is 36° to the southeast and is thought to represent the dip of the postglacial fault at this locality. Along the whole extension of the Stouragurra Fault, the downthrown side is to the northwest.

Two benchmarks for levelling have been established in bedrock on either side of the fault (90 m distance across the fault). The benchmarks are located 250 m to the north of the small lake (see section above and Figs. 24 & 25). Precision levelling by the Norwegian Mapping

Authority (SK) in 1987 and 1991 revealed a vertical displacement of 2.3±0.8 mm (Fig. 26) which is statistically significant at a level better than 95%. Benchmarks for GPS-measurements were established at the same locations in 1997 (Fig. 27).

Walk 2 km along the fault escarpment to the northernmost end and continue for 500 m due north to hit another fault section. The two parallel fault sections make up an en echelon appearance of the SF. (This feature is also typical at other locations.) In the hanging wall block of this northern section of the SF (UTM 604600-7710400) a 30 m long, 1 m wide and 1 m deep trench occurs sub-parallel to the escarpment (Fig. 28). The distance from the slightly curved trench to the escarpment is 40 m. The trench is most likely an accommodation fault formed during the postglacial faulting along a fault surface which is not planar.

An outcrop further north along the same fault segment has been sampled for AMS measurement and shows a dip of 49° to the southeast.

Figure 25. Oblique aerial photograph of the Stuoragurra postglacial fault to the north of Masi looking SW (Location 5) shown in Fig. 18 (UTM 604500-7709000). The SF starts immediately to the north of the lake and continues for 2 km to the NNE. The fault is easily assessable along path (around the lake) marked by the small arrows. Precision levelling is carried out across the fault 250 m to the north of the lake. The distance between the benchmarks (marked by the large arrows on either side of the fault) is 90 metres. Benchmarks for GPS measurements were installed at the same outcrops in 1997. The Kautokeino River and some houses in Masi can be seen in the background.

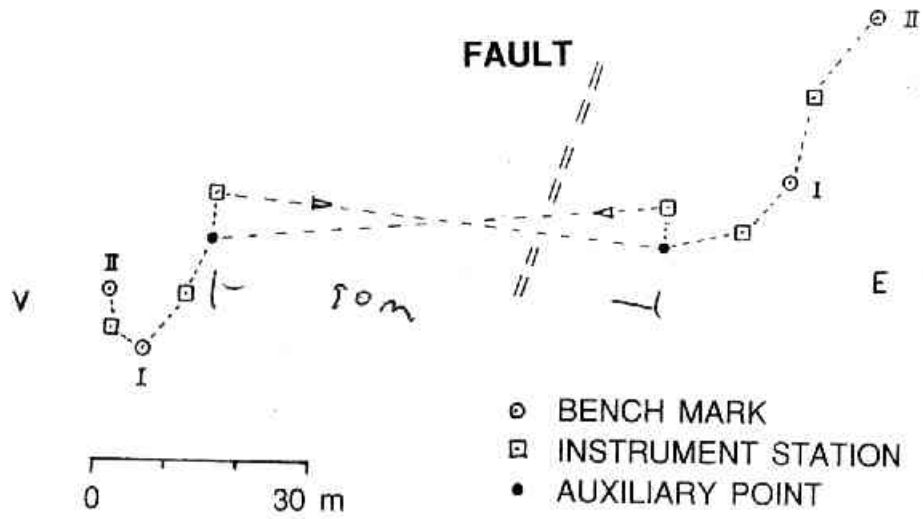

Uplift of hanging wall block:
2.3 mm ± 0.8 mm

Figure 26. Repeated precision levelling in 1987 and 1991 (from Skjøthaug 1991).

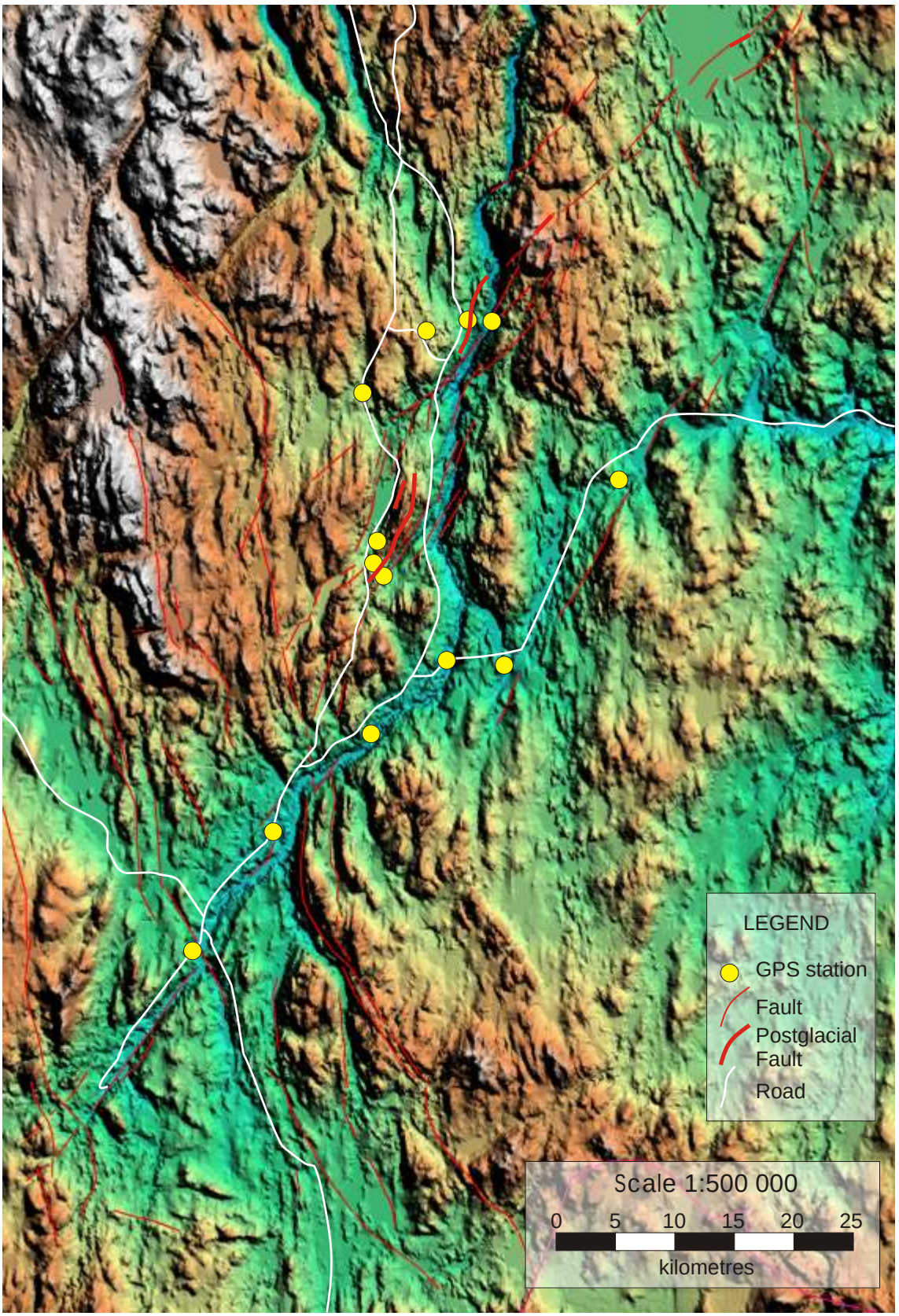

Figure 27. Locations of the GPS stations setup around the Stuoragurra postglacial fault during the summer of 1997.

Figure 28. A 30 m long, 1 m wide and 1 m deep trench sub-parallel to the escarpment in the hanging-wall block of the SF (UTM 604600-7710400). View towards the SW. The trench is most likely an accommodation fault formed during the postglacial faulting along a fault surface which is not planar.

3. REFERENCES

Bungum, H. & Lindholm, C. 1997: Seismo- and neotectonics in Finnmark, Kola Peninsula and the southern Barents Sea, part 2: Seismological analysis and seismotectonics. Tectonophysics 270, 15-28.

Corner, G.D., Yevzerov, V.Y., Kolka, V.V. & Møller, J.J. 1999: Isolation basin stratigraphy and Holocene relative sea-level change at the Norwegian-Russian border north of Nikel, northwest Russia. Boreas 28, 146-166.

Corner, G.D. 1972: Rockslides in North Norway, Norway. Unpublished report Tromsø museum, 10 pp.

Dehls, J. & Braathen, A. 1998: Neotectonic phenomena in southern Norway. In: Dehls, J. & Olesen, O. 1998 (eds.) Neotectonics in Norway, Annual Technical Report 1997, NGU Report 98.016, 31-39.

Hovland, M. 1983: Elongated depressions associated with pockmarks in the western slope of the Norwegian Trench. *Marine Geology 50*, M11-M20.

Hovland, M. & Judd, A.G., 1988: *Seabed pockmarks and seepages.* Graham & Trotman, London, 293 pp.

Jibson, R.W. 1994: Using landslides for Paleoseismic analysis. In McCalpin, (ed.): Paleoseismology. International geophysics series 62, 397-438. Academic press.

Keefer, D.K. 1984: Landslides caused by earthquakes. Geological Society of America Bulletin 95, 406-421.

Kakkuri, J. & Chen, R. 1992: On horizontal crustal strain in Finland. BULLETIN Géodésique 66, 12-20.

Keefer, D.K. 1984: Landslides caused by earthquakes. Geological Society of America Bulletin 95, 406-421.

Klementsrud, T. & Hilmo, B.O. 1999: Groundwater studies in the Stuoragurra Fault. In: Dehls, J. & Olesen, O. 1999 (eds.) Neotectonics in Norway, Annual Technical Report 1998, NGU Report 99.007, 143-145.

Krill, A.G., Bergh, S., Lindahl, I. Mearns, E.W., Often, M., Olerud, S., Olesen, O., Sandstad, J.S., Siedlecka, A., & Solli, A. 1985: Rb-Sr, U-Pb and Sm-Nd isotopic dates from Precambrian rocks of Finnmark. Nor. geol. unders. Bull. 403, 37-54.

Kuivamäki, A, Vuorela, P. & Paananen, M. 1998: Indications of postglacial and recent bedrock movements in Finland and Russian Karelia. Geological Survey of Finland Report YST-99, 97 pp.

Kujansuu, R., 1964. Nuorista sirroksista Lapissa. Summary: Recent faults in Lapland. Geologi, 16: 30-36.

Lagerbäck, R., 1979. Neotectonic structures in northern Sweden. Geologiska Föreningens i Stockholm Förhandlingar, 100 (1978), 271-278.

Lagerbäck, R. 1990: Late Quaternary faulting and paleoseismicity in northern Fennoscandia, with particular reference to the Lansjärv area, northern Sweden. Geologiska Föreningens i Stockholm Förhandlingar 112, 333-354.

Lundquist, J. & Lagerbäck, R. 1976: The Pärve Fault: A late-glacial fault in the Precambrian of Swedish Lapland. Geol. Fören. Stockh. Förh. 98, 45-51.

Marthinussen, M. 1974: Contributions to the Quaternary geology of north-easternmost Norway and closely adjoining foreign territories. Nor. Geol. Unders. Bull. 315, 157 pp.

Mauring, E., Olesen, O., Rønning J.S & Tønnesen, J.F. 1997: Ground-penetrating radar profiles across postglacial faults at Kåfjord, Troms and Fidnajohka, Finnmark. NGU Report 97.174, 16 pp.

Mauring, E., Rønning J.S & Dehls, J.F. 1999: Ground-penetrating radar profiles across postglacial faults at Kåfjord (Troms), Masi (Finnmark) and Sodankylä, Finland. In: Dehls, J. & Olesen, O. 1999 (eds.) Neotectonics in Norway, Annual Technical Report 1998, NGU Report 99.007, 115-124.

Muir Wood, R., 1989. Extraordinary deglaciation reverse faulting in northern Fennoscandia. In: S. Gregersen and P.W. Basham (Editors) Earthquakes at North-Atlantic passive margins: neotectonics and postglacial rebound. NATO ASI series. Series C, Mathematical and physical sciences, Vol. 266. Kluwer Academic Publishers, Dordrecht, pp. 141-173.

Muir Wood, R. 1993: A review of the seismotectonics of Sweden. Swedish Nuclear Fuel and Waste Management Co. Technical Report 93-13, 225 pp.

Muir Wood, R. & King, G.C.P. 1993: Hydrological signatures of earthquake strain. Journ. Geophys. Research 98, 22,035-22,068.

Olesen, O., 1988. The Stuoragurra Fault, evidence of neotectonics in the Precambrian of Finnmark, northern Norway. Nor. Geol. Tidsskr., 68: 107-118.

Olesen, O. 1991: A geophysical investigation of the relationship between old fault structures and postglacial faults in Finnmark, northern Norway. Unpubl. Dr. ing. thesis. 1991:54, University of Trondheim, Norwegian Institute of Technology. 126 pp.

Olesen, O. & Dehls, J. 1998: Neotectonic phenomena in northern Norway. In: Dehls, J. & Olesen, O. 1998 (eds.) Neotectonics in Norway, Annual Technical Report 1997, NGU Report 98.016, 3-30.

Olesen, O. & Sandstad, J. S., 1993: Interpretation of the Proterozoic Kautokeino Greenstone Belt, Finnmark, Norway from combined geophysical and geological data. *NGU Bulletin* 425.

Olsen, L., Dehls, J.F., Olesen, O. & Rønning J.S. 1999: Late Quaternary faulting and paleoseismicity in Finnmark, northern Norway. In: Dehls, J. & Olesen, O. 1999 (eds.) Neotectonics in Norway, Annual Technical Report 1998, NGU Report 99.007, 93-102.

Olesen, O., Henkel, H., Lile, O.B., Mauring, E. & Rønning J.S. in 1992a: Geophysical investigations of the Stuoragurra postglacial fault, Finnmark, northern Norway. Journal of Applied Geophysics 29, 95-118.

Olesen, O., Henkel, H., Lile, O.B., Mauring, E., Rønning, J.S. & Torsvik, T.H. 1992b: Neotectonics in the Precambrian of Finnmark, northern Norway. Norsk Geol. Tidsskr. 72 301-306.

Olesen, O., Roberts, D., Henkel, H., Lile, O.B. and Torsvik, T. H., 1990. Aeromagnetic and gravimetric interpretation of regional structural features in the Caledonides of West Finnmark and North Troms, northern Norway. Nor. geol. unders. Bull., 419: 1-24.

Olesen, O., Roberts, D. & Olsen, L. 1992c: Neotectonic studies in Finnmark 1992. NGU Rapport 92.325, 15 s.

Riis, F. 1996: Quantification of Cenozoic vertical movements of Scandinavia by correlation of morphological surfaces with offshore data. *Global and Planetary Change 12*, 331-357.

Roberts, D., 1991. A contemporary small-scale thrust-fault near Lebesby, Finnmark. Norsk Geol. Tidsskr. 71, 117-120.

Roberts, D., Olesen, O. & Karpuz, M.R. 1997: Seismo- and neotectonics in Finnmark, Kola Peninsula and the southern Barents Sea. Part I: Geological and neotectonic framework. Tectonophysics 270, 1-13.

Sibson, R.H. 1981: Fluid flow accompanying faulting: field evidence and models. In: D.W. Sinmpson & P.G. Richards (eds.). Earthquake prediction: an International Review. Maurice Ewing Series 4, Am. Geophys. Union, Washington D.C., 593-603.

Siedlecka, A. & Roberts, D. 1996: Finnmark Fylke. Berggrunnsgeologi M 1:500 000. Nor. geol. unders., Trondheim.

Skjøthaug, P. 1991: Rapport fra nivellement over Stuoragurrafrokastningen 1991. Norwegian Mapping Authority (Statens kartverk) Report, 2 pp.

Solli, A., 1988. Masi 1933 IV - berggrunnsgeologisk kart - M 1:50 000. Nor. geol. unders., Trondheim.

Sollid, J.L. & Tolgensbakk, J. 1988: Kvartærgeologisk og geomorfologisk kartlegging på Svalbard og fastlands-Norge utført ved Geografisk Institut, Univ. i Oslo. Abstract 18th Nordic Geological Meeting, Copenhagen, 380-381.

Stuevoll, L.M. & Eldholm, O. 1996: Cenozoic uplift of Fennoscandia inferred from a study of the mid-Norwegian margin. *Global and Planetary Change 12*, 359-386.

Tanner, V., 1907: Studier öfer kvartärsystemet i Fennoskandias nordliga delar. I: Till frågan om Ost-Finmarkens glaciation och nivåförändringar. Résymé en francais. *Bull. Comm. Géol. Finl. 18*, 165 p

Tolgensbakk, J. & Sollid, J.L. 1988: Kåfjord, kvartærgeologi og geomorfologi 1:50 000, 1634 II. Geografisk institutt, Universitetet i Oslo.

Varnes, D.J., Radbruch-Hall, D.H. & Savage, W.Z. 1989: Topographic and structural conditions in areas of gravitional spreading of ridges in the western United States. U.S. Geological Survey Professional Paper 1496, 28 pp.

Wells, D. L. and Coppersmith, K.J. 1994: Empirical relationships among magnitudes, rupture length, rupture area and surface displacement. *Bull. Seismol. Soc. Am. 82*, 1756-1784.

Yevzerov, V.Y., Møller, J.J., Kolka, V.V. & Corner, G.D. 1998: Marine beach-ridges of Rybachi and Sredni peninsulas, northwest Russia: indicators of deglatiation and uplift. 2nd QUEEN workshop, St. Petersburg, 6-9 Feb. (abstract).